Short Communication

Tutorial on Fourier Transform for Ultrafast Optics

Yi-Hao Chen[1]

1. School of Applied and Engineering Physics, Cornell University, United States

This tutorial is designed for individuals who are new to the field of ultrafast optics. It was written in response to the apparent lack of comprehensive introductions to the basic Fourier transform, extending beyond the flat-phase description. Additionally, there is a need for complete derivations of several relations involving the Fourier transform, maintaining its most general formulation. This approach avoids the arbitrary selection of Fourier-transform constants and ensures a complete understanding. It shows the importance of having Fourier-transform constants as parameters, which I would like to advocate people to do. Most important of all, I have seen misuse of Fourier transform over my years of discussion in the lab and from others' questions since I shared my code publicly on Github. Surprisingly, since people check the correctness of numerical implementation only by seeing if the simulation result is smooth and if it duplicates the "overall physics," this seems to be a widespread problem from my perspective, which can be solved by a simple tutorial (see Sec. 2B). This is why I hope that this tutorial can help people understand more about the Fourier transform, especially in the context of ultrafast optics.

Feel me to send me an email if there is any confusion, or you think that there is more to add to this tutorial.

Corresponding author: Yi-Hao Chen, yc2368@cornell.edu

1. Analytic signal

A. Introduction

When we learn ultrafast optics with textbooks, such as Boyd's Nonlinear Optics[1], they usually start with the field equation for the real-valued field:

$$\begin{aligned}\mathbf{E}(t) &= \frac{1}{2}\left(\mathcal{E}(t)+\mathcal{E}^*(t)\right) = \frac{1}{2}\left(E(t)e^{-i\omega_0 t}+E^*(t)e^{i\omega_0 t}\right)\\ &= \mathrm{Re}\left[\mathcal{E}(t)\right]\end{aligned} \tag{S1}$$

or simply assume, for the complex-valued field:

$$\mathcal{E}(t) = E(t)e^{-i\omega_0 t}. \tag{S2}$$

These two equations make intuitive sense if the field is a simple sinusoidal wave that follows $\mathbf{E}(t)=\sin(\omega_0 t)=\frac{e^{i\omega_0 t}-e^{-i\omega_0 t}}{2i}$ so that the coefficient $E(t)$ in Eq. (S1) is just $\frac{-1}{2i}$. However, in general situations of real-valued $\mathbf{E}(t)$, there are infinite possible options for complex-valued $\mathcal{E}(t)$ that satisfies Eq. (S1). During nonlinear studies, there are usually conversions between temporal and spectral components through the Fourier transform. Not correctly defining or understanding the decomposition of the field following the form of Eq. (S1) can not only result in a mixed use of Fourier transform of the real-valued $\mathbf{E}(t)$ and complex-valued $\mathcal{E}(t)$ (which will be discussed in detail in Fig. S1) but also mislead researchers from obtaining all generated frequencies, leading to the problem with missing negative frequencies[2]. Therefore, it is important to understand and apply

 doi.org/10.32388/JFPRSL

the correct decomposition. Here I will introduce the "analytic-signal decomposition," which decomposes the real-valued signal into its positive- and negative-frequency components. The positive-frequency part is called the "analytic signal," whose complex conjugate is the negative-frequency part of the real-valued signal.

An analytic signal is a complex-valued function that has no negative-frequency part. If $s(t)$ is a real-valued function with Fourier transform $\mathfrak{F}[s] = S(f)$, then it exhibits the Hermitian symmetry about $\nu = 0$.

$$S(-\nu) = S^*(\nu). \tag{S3}$$

Thus, there is redundancy if both frequencies are considered; negative-frequency components can be discarded without loss of information.

We define $S_a(\nu)$ to represent the positive-frequency part as the following:

$$\begin{aligned} S_a(\nu) &= \begin{cases} 2S(\nu), & \nu > 0 \\ S(\nu), & \nu = 0 \\ 0, & \nu < 0 \end{cases} \\ &= S(\nu) + \nu S(\nu), \end{aligned} \tag{S4}$$

so that

$$\begin{aligned} S(\nu) &= \begin{cases} \frac{1}{2} S_a(\nu), & \nu > 0 \\ S_a(\nu), & \nu = 0 \\ \frac{1}{2} S_a^*(-\nu), & \nu < 0 \end{cases} \\ &= \frac{1}{2}\left(S_a(\nu) + S_a^*(-\nu)\right) \end{aligned} \tag{S5}$$

and thus

$$s(t) = \frac{1}{2}\left(s_a(t) + s_a^*(t)\right). \tag{S6}$$

$s(t)$ is a combination of its analytic signal $s_a(t)$ and the corresponding complex conjugate, which is the negative-frequency part of the $s(t)$.

Since analytic signal of $s(t)$ is the inverse Fourier transform of $S_a(\nu)$,

$$\begin{aligned} s_a(t) &= \mathfrak{F}^{-1}\left[S(\nu) + \nu S(\nu)\right] \\ &= s(t) + C_{\mathfrak{F}} \mathfrak{F}^{-1}\left[\nu\right] * \mathfrak{F}^{-1}\left[S(\nu)\right] \quad \text{with the convolution theorem [Eq. (S10a)]} \\ &= s(t) + C_{\mathfrak{F}}\left[\left(C_{\mathfrak{I}\mathfrak{F}} c_s \frac{2}{it}\right) * s(t)\right] \quad \because \mathfrak{F}^{-1}\left[f\right] = C_{\mathfrak{I}\mathfrak{F}} c_s \frac{2}{it} \\ &= s(t) + \left[\left(-\frac{ic_s}{\pi t}\right) * s(t)\right], \because C_{\mathfrak{F}} C_{\mathfrak{I}\mathfrak{F}} = \frac{1}{2\pi} \end{aligned} \tag{S7}$$

Any real-valued signal can be decomposed into its positive-frequency (analytic-signal) and negative-frequency parts, which underlies the decomposition of Eq. (S1). In addition, this tells us that the Fourier transform of the real-valued field $\mathbb{E}(t)$ is different from that of the analytic signal $\mathcal{E}(t)$; they exhibit different spectral components. Hence, it is crucial to define clearly what is being used, especially in studies of, for example, four-wave mixing and Raman scattering that involves nonlinear evolutions of different frequencies. In principle, any derivations of nonlinear optics should start with the real-valued signal, followed by its decomposition into the "analytic signal." If a derivation starts directly with a single complex-valued signal (either the positive- or negative-frequency part), then readers need to be cautious about two things: (1) whether there is any missing frequency component due to ignoring the complex-conjugate part, and (2) whether there is a deviation of a factor of 2. As an example,[3] starts with the complex-valued field for deriving the Raman-induced index change, which eventually results in a reported deviation of a factor of 2 between their theory and experiments. (Correct derivation with analytic signal,

as well as generalization to an arbitrary polarization, is in[4].) As another example, the third-order nonlinear polarization $\vec{\mathbb{P}}(t) = \int_{-\infty}^{\infty} \chi^{(3)}(t_1,t_2,t_3) \vdots \vec{\mathbb{E}}(t-t_1)\vec{\mathbb{E}}(t-t_2)\vec{\mathbb{E}}(t-t_3)dt_1dt_2dt_3$ is apparently different from $\vec{\mathcal{P}}'(t) = \int_{-\infty}^{\infty} \chi^{(3)}(t_1,t_2,t_3) \vdots \vec{\mathcal{E}}(t-t_1)\vec{\mathcal{E}}(t-t_2)\vec{\mathcal{E}}(t-t_3)dt_1dt_2dt_3$, as $\vec{\mathcal{P}}'(t)$ lacks all frequency components that result from combinations including the negative-frequency components of three $\vec{\mathbb{E}}(t)$'s. Therefore, $\vec{\mathcal{P}}'(t)$ is not the correct calculation for the analytic signal $\vec{\mathcal{P}}(t)$ of $\vec{\mathbb{P}}(t)$. A correct $\vec{\mathcal{P}}(t)$ should be calculated by identifying the positive-frequency part of $\vec{\mathbb{P}}(t) = \frac{1}{2}\left(\vec{\mathcal{P}}(t) + \vec{\mathcal{P}}^*(t)\right) = \int_{-\infty}^{\infty} \chi^{(3)}(t_1,t_2,t_3) \vdots \vec{\mathbb{E}}(t-t_1)\vec{\mathbb{E}}(t-t_2)\vec{\mathbb{E}}(t-t_3)dt_1dt_2dt_3$.

B. Offset frequency $\Omega = \omega - \omega_0$

Applying analytic signal provides benefits in numerical computations. Because real-valued signal contains both positive and negative frequencies, its frequency window should cover both signs of frequency [Fig. S1(a)]. By extracting ω_0 out as in Eq. (S1), the Fourier transform of $E(t)$ (to obtain $E(\Omega) = \mathfrak{F}[E] = C_{\mathfrak{F}} \int_{-\infty}^{\infty} E(t) e^{ic_s \Omega t} dt$ [Eq. (S8)]) is equivalent to applying it with respect to the offset frequency $\Omega = \omega - \omega_0$ [Fig. S1(b)]. The offset center of the frequency window, from $\omega = 0$ to ω_0, enables a small window covering only around the signal's spectrum, free from the redundant negative-frequency components. As an example, a broadband simulation of a Yb-doped fiber laser requires a 100-THz window to cover signals from 1–1.2 μm without inducing aliasing.[1] On the other hand, the frequency window of the real-valued $\mathbb{E}(t)$ should be $\sim$ 700-THz wide for a 1-μm ($\approx$ 300 THz) pulse (if we assume the same 100-THz coverage around the signal: $700 = 2 \times 300 + 100$). If ω_0 is the pulse's center frequency, $E(t)$ is called the "slowly-varying" envelope of $\mathcal{E}(t)$. $E(t)$ can be real-valued if the analytic signal $\mathcal{E}(t)$ exhibits no extra phase variation other than sinusoidal waves. Thus, the frequency window of the analytic signal's envelope is 7 times smaller than that of the real-valued signal, allowing a numerical simulation with a larger temporal sampling period and thus less sampling points. For narrowband simulations, the computational improvement can be more significant (an improvement factor of $\frac{600+x}{x}$ with a small x, the size of the narrowband-signal's frequency window). In general, ω_0 does not need to be at the pulse's center frequency. For broadband nonlinear processes such as vibrational-Raman generation in H_2 that creates frequency 125 THz apart from the pump frequency[5][6], or $\geq$ 250 THz for cascaded processes[7][8], ω_0 should be placed such that the frequency window can cover all generated frequency components.

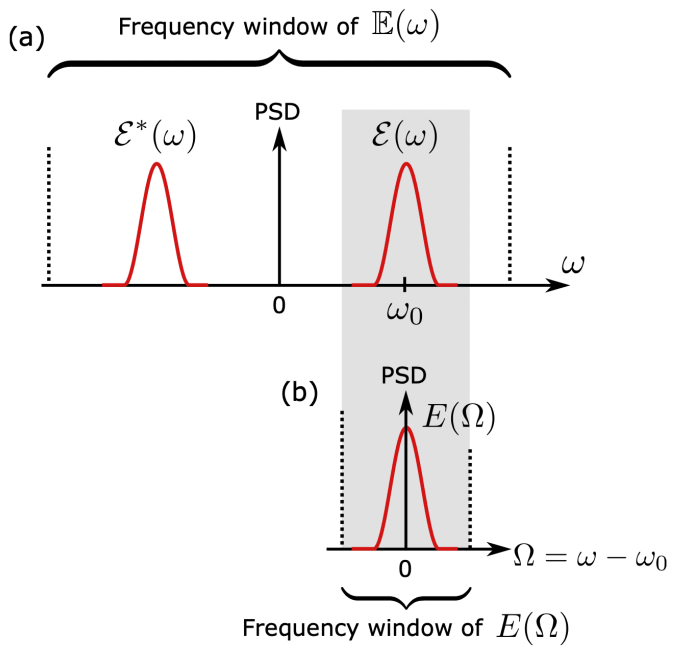

Figure S1. Spectral domain of the Fourier-transform components of (a) the real-valued signal and (b) the envelope of its analytic signal [Eq. (S1)]. PSD: power spectral density $\sim \mathfrak{F}[\cdot]^2$

2. Spectral Fourier transform

In this section, we explain the Fourier transform in its continuous and discrete formats. In addition, all constants are represented as parameters to be compatible with various conventions people in different fields use. I would also like to advocate people to derive their equations based on parametrized Fourier transform, as in Eq. (S8). As I will show later, many relations are dependent on the Fourier-transform convention and its constants. Various conventions out there in the world (e.g., $C_{\mathfrak{F}} = 1$ or $C_{\mathfrak{F}} = \frac{1}{\sqrt{2\pi}}$ [Eq. (S8)]) can create misleading equations. For example, if an equation has π, we do not know whether it is dependent on Fourier-transform constants or not; it can come from anywhere, such as the frequency relation $\omega = 2\pi\nu$ that is irrelevant to Fourier transform. Furthermore, losing the information of Fourier-transform constants prevents people from correctly transforming the equation from continuous to discrete Fourier transform for numerical computations, as I would show later in Sec. 2C.

Here in this tutorial, the overall trend of notation follows the physical convention whose inverse spectral Fourier transform follows $A(t) \sim \int A(\omega) e^{i(k_z z - \omega t)} d\omega$, which is the spectral Fourier transform in mathematics or engineering. Note that in contrast to the spectral Fourier transform, the physical convention ($k_z z - \omega t$) potentially shows that the spatial Fourier transform $\mathfrak{F}_{k_z}$ is consistent with mathematical convention; however, we typically do not calculate based on the k_z-space. Here, we will focus only on spectral Fourier transform.

A. Definition

In general, the Fourier transform is defined as

doi.org/10.32388/JFPRSL

$$
\begin{aligned}
A(\omega) &= \mathfrak{F}[A(t)] \equiv C_{\mathfrak{F}} \int_{-\infty}^{\infty} A(t) e^{i c_s \omega t} dt \\
A(t) &= \mathfrak{F}^{-1}[A(\omega)] \equiv C_{\mathfrak{IF}} \int_{-\infty}^{\infty} A(\omega) e^{-i c_s \omega t} d\omega.
\end{aligned}
\tag{S8}
$$

If $c_s = 1$, the Fourier transform follows the physical convention; whereas it follows the mathematical convention if it is -1. Its constants satisfy $C_{\mathfrak{F}} C_{\mathfrak{IF}} = \frac{1}{2\pi}$, which is found with

$$
\begin{aligned}
A(t) &= C_{\mathfrak{IF}} \int_{-\infty}^{\infty} A(\omega) e^{-i c_s \omega t} d\omega \\
&= C_{\mathfrak{IF}} \int_{-\infty}^{\infty} \left(C_{\mathfrak{F}} \int_{-\infty}^{\infty} A(\tau) e^{i c_s \omega \tau} d\tau \right) e^{-i c_s \omega t} d\omega \\
&= C_{\mathfrak{F}} C_{\mathfrak{IF}} \int_{-\infty}^{\infty} \int_{-\infty}^{\infty} A(\tau) e^{i c_s \omega (\tau - t)} d\omega d\tau \\
&= C_{\mathfrak{F}} C_{\mathfrak{IF}} \int_{-\infty}^{\infty} A(\tau) \frac{2\pi}{|c_s|} \delta(\tau - t) d\tau \\
&= C_{\mathfrak{F}} C_{\mathfrak{IF}} A(t) 2\pi \quad \because |c_s| = 1 \\
\Rightarrow C_{\mathfrak{F}} C_{\mathfrak{IF}} &= \frac{1}{2\pi}.
\end{aligned}
\tag{S9}
$$

Since the convolution theorem is a commonly-used relation, we show it below:

$$
\mathfrak{F}[A * B] = \frac{1}{C_{\mathfrak{F}}} \mathfrak{F}[A] \mathfrak{F}[B] \tag{S10a}
$$

$$
\mathfrak{F}^{-1}[A * B] = \frac{1}{C_{\mathfrak{IF}}} \mathfrak{F}^{-1}[A] \mathfrak{F}^{-1}[B]. \tag{S10b}
$$

The discrete counterpart is

$$
\begin{aligned}
\mathfrak{F}_{D_c}[A * B] &= \frac{1}{C_{\mathfrak{F}}} \mathfrak{F}_{D_c}[A] \mathfrak{F}_{D_c}[B] \\
\mathfrak{F}_{D_c}^{-1}[A * B] &= \frac{1}{C_{\mathfrak{IF}}} \mathfrak{F}_{D_c}^{-1}[A] \mathfrak{F}_{D_c}^{-1}[B]
\end{aligned}
\quad \text{if} \quad
\begin{aligned}
A(\omega) &= \mathfrak{F}_{D_c}[A(t_n)] \equiv C_{\mathfrak{F}} \sum_{n=1}^{\mathfrak{N}} A(t_n) e^{i c_s \omega t_n} \triangle t \\
A(t) &= \mathfrak{F}_{D_c}^{-1}[A(\omega_m)] \equiv C_{\mathfrak{IF}} \sum_{m=1}^{\mathfrak{N}} A(\omega_m) e^{-i c_s \omega_m t} \triangle \omega
\end{aligned}
. \tag{S11}
$$

$\mathfrak{F}$ and $\mathfrak{F}_{D_c}$ are the continuous and discrete versions of Fourier transform, respectively. $\mathfrak{N}$ is the number of discrete points. In the discrete manner, $t_n = n\Delta t$ and $\omega_m = m\Delta\omega$. The time window is $T^w = \mathfrak{N}\Delta t$, and the frequency window $\nu^w = \frac{1}{\Delta t} = \frac{\mathfrak{N}}{T^w} = \mathfrak{N}\Delta\nu$. The angular-frequency spacing $\Delta w = 2\pi\Delta\nu = \frac{2\pi}{T^w}$. If the sampling frequency is high enough, $\mathfrak{F}_{D_c}[\cdot] \approx \mathfrak{F}[\cdot]$ and $\mathfrak{F}_{D_c}^{-1}[\cdot] \approx \mathfrak{F}^{-1}[\cdot]$.

In practice, during numerical computations, we sloppily treat the result from the following discrete Fourier transform (DFT) simply as Fourier transform:

$$
\begin{aligned}
A_D(\omega) &= \mathfrak{F}_D[A(t_n)] \equiv C_{\mathfrak{F}_D} \sum_{n=1}^{\mathfrak{N}} A(t_n) e^{i c_s \omega t_n} \\
A(t) &= \mathfrak{F}_D^{-1}[A_D(\omega_m)] \equiv C_{\mathfrak{IF}_D} \sum_{m=1}^{\mathfrak{N}} A_D(\omega_m) e^{-i c_s \omega_m t},
\end{aligned}
\tag{S12}
$$

which differs from the Fourier transform [Eq. (S11)] in constants and units:

$$
\mathfrak{F} = \frac{C_{\mathfrak{F}}}{C_{\mathfrak{F}_D}} \Delta t \mathfrak{F}_D \tag{S13a}
$$

$$
\mathfrak{F}^{-1} = \frac{C_{\mathfrak{IF}}}{C_{\mathfrak{IF}_D}} \Delta\omega \mathfrak{F}_D^{-1}. \tag{S13b}
$$

If we replace variables following $\omega_m = m\Delta\omega = m\frac{2\pi}{T^w} = m\frac{2\pi}{\mathfrak{N}\Delta t}$ and $t_n = n\Delta t$, Eq. (S12) becomes

$$
\begin{aligned}
A_D(\omega_m) &= \mathfrak{F}_D[A(t_n)] \equiv C_{\mathfrak{F}_D} \sum_{n=1}^{\mathfrak{N}} A(t_n) e^{ic_s \frac{2\pi}{\mathfrak{N}} mn} \\
A(t_n) &= \mathfrak{F}_D^{-1}[A_D(\omega_m)] \equiv C_{\mathfrak{I}\mathfrak{F}_D} \sum_{m=1}^{\mathfrak{N}} A_D(\omega_m) e^{-ic_s \frac{2\pi}{\mathfrak{N}} nm},
\end{aligned}
\tag{S14}
$$

where $C_{\mathfrak{F}_D} C_{\mathfrak{I}\mathfrak{F}_D} = \frac{1}{\mathfrak{N}}$, found with the similar process to Eq. (S9).

The DFT $A_D(\omega)$ [Eq. (S12)] is denoted with an extra "D" subscript to distinguish it from $A(\omega)$ of Eqs. (S8) and (S11). Therefore, it is important to derive a relationship between $A(\omega)$ and $A_D(\omega)$, which follows

$$
\frac{1}{C_{\mathfrak{F}_D}} A_D(\omega) \Delta t = \frac{1}{C_{\mathfrak{F}}} A(\omega)
\tag{S15}
$$

so that they obtain the same $A(t)$. For the commonly-used Fourier-transform convention in the laser field (and the one we emphasize in this article), $c_s = 1$ so that the inverse Fourier transform is consistent with the use of $A(t) \sim \int A(\omega) e^{i(k_z z - \omega t)} d\omega$ in physical representation. With this convention, the inverse Fourier transform in mathematics becomes the Fourier transform in physics, so we define $C_{\mathfrak{F}_D} = \frac{1}{\mathfrak{N}}$, the constant of the mathematical inverse DFT, such that Eq. (S15) becomes $A_D(\omega) = A(\omega)\Delta\nu / C_{\mathfrak{F}}$ in this convention.

B. Important correct application of the Fourier-transform convention

Many physics equations are derived by assuming that the phase follows $(k_z z - \omega t)$, which implies that the Fourier transform in physics is the inverse Fourier transform in mathematics, i.e., $c_s = 1$. For example in unidirectional pulse propagation equation:

$$
\begin{aligned}
\partial_z A_p(z,\Omega) = & \, i\left[\beta_p(\omega) - \left(\beta_{(0)} + \beta_{(1)}\Omega\right)\right] A_p(z,\Omega) \\
& + i\frac{\omega n_2}{c} \sum_{\ell mn} \Bigg\{ (1 - f_R)\, S^K_{p\ell mn} \mathfrak{F}\left[A_\ell A_m A_n^* + \tilde{\Gamma}^K_{p\ell mn} \right. \\
& + f_R \left\{ f_a S^{R_a}_{p\ell mn} \mathfrak{F}\left[A_\ell \left\{ h_a(t) * \left[A_m A_n^* + \tilde{\Gamma}^{R_a}_{p\ell mn} \right] \right\} \right] \right. \\
& \left. \left. + f_b S^{R_b}_{p\ell mn} \mathfrak{F}\left[A_\ell \left\{ h_b(t) * \left[A_m A_n^* + \tilde{\Gamma}^{R_b}_{p\ell mn} \right] \right\} \right] \right\} \Bigg\},
\end{aligned}
\tag{S16}
$$

where the explanation of notations can be found in [9]. Its derivation can be found in the supplement of [4] and we can see that A_p results from

$$
\vec{\mathbb{E}}(\vec{r},t) = \sum_p \int d\omega \frac{1}{2} \left\{ \frac{\vec{F}_p(\vec{r}_\perp,\omega)}{N_p(\omega)} A_p(z,\omega) e^{i[\beta_p(\omega) z - \omega t[} + \text{c.c.} \right\},
\tag{S17}
$$

where A_p represents the envelope of the analytic signal of the real-valued electric field $\vec{\mathbb{E}}(\vec{r},t)$. Some might rewrite it in the time domain (with a narrowband assumption with Taylor-series expansion around center frequency ω_0) as

$$
\begin{aligned}
\partial_z A_p(z,T) = & \left\{ i\left[\beta_p^{(0)}(\omega_0) - \beta_{(0)}\right] - \left[\beta_p^{(1)}(\omega_0) - \beta_{(1)}\right] \partial_T \right\} A_p(z,T) + i \sum_{m\geq 2} \frac{(i\partial_T)^m}{m!} \beta_p^{(m)}(\omega_0) A_p(z,T) \\
& + \frac{i\omega_0 n_2}{c} \left[1 + \tau_{p\ell mn}\,(i\partial_t)\right] \sum_{\ell mn} \Bigg\{ (1 - f_R)\, S^K_{p\ell mn} \left[A_\ell A_m A_n^* + \tilde{\Gamma}^K_{p\ell mn} \right] \\
& + f_R \left\{ f_a S^{R_a}_{p\ell mn} \left[A_\ell \left\{ h_a(t) * \left[A_m A_n^* + \tilde{\Gamma}^{R_a}_{p\ell mn} \right] \right\} \right] + f_b S^{R_b}_{p\ell mn} \left[A_\ell \left\{ h_b(t) * \left[A_m A_n^* + \tilde{\Gamma}^{R_b}_{p\ell mn} \right] \right\} \right] \right\} \Bigg\},
\end{aligned}
\tag{S18}
$$

intending to be free from spectral computations. Still, terms with $i\partial_T A(z,T)$ that results from $\Omega A(z,\Omega)$ are related to the convention of Fourier transform with $c_s = 1$:

$$
\partial_T A(z,T) \overset{\mathfrak{F}}{\to} -ic_s \Omega A(z,\Omega).
\tag{S19}
$$

As a result, it is crucial to apply the correct Fourier-transform convention. In nonlinear optics, it follows the physical convention; i.e., use mathematical (MATLAB's) fft for Fourier transform into the spectral domain and use mathematical (MATLAB's) fft for inverse Fourier transform into the temporal domain. Some might think that, in numerical computations, the wrong use of Fourier transform simply creates a signal that is a complex conjugate of the correct one, both following the same pulse propagation equation. Since the analytic signal, or its envelope, is generally complex-valued, the spectral signal transformed with mathematical fft is not a complex conjugate of the spectral signal transformed with mathematical ifft. Since $A(z,\Omega)$ is the envelope centering around ω_0 [Fig. S1], the wrong convention represents the field of the reversed frequency sign $A(z,-\Omega)$ that should not follow the same pulse propagation equation as $A(z,\Omega)$. For example, the dispersion term $\beta(\omega)$ should be reversed around ω_0:

$$\beta(\omega=\omega_0+\Omega)\rightarrow\beta(\omega_0-\Omega). \tag{20}$$

In general, a wrong convention of Fourier transform applied to an equation derived with a different convention simply creates a wrong pulse-propagation result, unless the equation is revised accordingly.

C. Conversion of quantities with physically-useful units between FT and DFT

In this section, we derive several formulae for conversion of physical quantities between Fourier transform and discrete Fourier transform.

$$\begin{aligned}
\int_{-\infty}^{\infty}|A(t)^2|dt &= \int_{-\infty}^{\infty}C_{\mathfrak{IF}}^2\int_{-\infty}^{\infty}\int_{-\infty}^{\infty}A(\omega)A^*(\omega')e^{-ic_s(\omega-\omega')t}d\omega d\omega' dt \\
&= C_{\mathfrak{IF}}^2\int_{-\infty}^{\infty}\int_{-\infty}^{\infty}A(\omega)A^*(\omega')\left[\int_{-\infty}^{\infty}e^{-ic_s(\omega-\omega')t}dt\right]d\omega d\omega' \\
&= C_{\mathfrak{IF}}^2\int_{-\infty}^{\infty}\int_{-\infty}^{\infty}A(\omega)A^*(\omega')\left[2\pi\delta(c_s(\omega-\omega'))\right]d\omega d\omega' \\
&= 2\pi C_{\mathfrak{IF}}^2\int_{-\infty}^{\infty}|A(\omega)^2|d\omega, \quad \delta(c_s(\omega-\omega'))=\frac{\delta(\omega-\omega')}{|c_s|}=\delta(\omega-\omega') \\
&= \frac{C_{\mathfrak{IF}}}{C_{\mathfrak{F}}}\int_{-\infty}^{\infty}|A(\omega)^2|d\omega. \qquad \because C_{\mathfrak{IF}}=\frac{1}{2\pi C_{\mathfrak{F}}}
\end{aligned} \tag{S21}$$

Eq. (S21) leads to the general formulation of the Parseval's theorem:

$$\frac{1}{C_{\mathfrak{IF}}}\int_{-\infty}^{\infty}|A(t)^2|dt=\frac{1}{C_{\mathfrak{F}}}\int_{-\infty}^{\infty}|A(\omega)^2|d\omega. \tag{S22}$$

With Eq. (S15) and $\Delta\omega=\frac{2\pi}{\mathfrak{N}\Delta t}$, we can derive the discrete version of the Parseval's theorem:

$$\frac{1}{C_{\mathfrak{IF}_D}}\sum_{n=1}^{\mathfrak{N}}|A(t_n)|^2=\frac{1}{C_{\mathfrak{F}_D}}\sum_{m=1}^{\mathfrak{N}}|A_D(\omega_m)|^2. \tag{23}$$

Rewriting the Parseval's theorem in powers leads to $\int_{-\infty}^{\infty}P(t)dt=\int_{-\infty}^{\infty}P(\omega)d\omega$, where $P(t)=|A(t)^2|$. Since $P(t)$ has the unit of "$\mathrm{W=J\ /\ s}$," $P(\omega)=\frac{C_{\mathfrak{IF}}}{C_{\mathfrak{F}}}|A(\omega)|^2=\frac{1}{2\pi C_{\mathfrak{F}}^2}|A(\omega)|^2$ has the unit of "$\mathrm{J\ /\ (rad\cdot Hz)}$" [$\omega$ has a unit of "$\mathrm{Hz\ /\ (2\pi)=rad\cdot Hz}$"]. To calculate the spectrum with the unit of "$\mathrm{\ J\ /\ Hz}$" numerically,

$$P(\nu)=2\pi P(\omega)=\frac{1}{C_{\mathfrak{F}}^2}|A(\omega)|^2=\left(\frac{\triangle\, t}{C_{\mathfrak{F}_D}}\right)^2|A_D(\omega)|^2, \tag{S24}$$

by applying Eq. (S15) and $C_{\mathfrak{F}}C_{\mathfrak{IF}}=\frac{1}{2\pi}$. $\int P(\omega)d\omega=\int P(\nu)d\nu$ leads to $P(\nu)=2\pi P(\omega)$. With the DFT convention we use here ($C_{\mathfrak{F}_D}=\frac{1}{\mathfrak{N}}$), it becomes $P(\nu)=(T^w)^2|A_D(\omega)|^2$.

The Parseval's theorem assumes the unit of energy (J) after the integral. However, for continuous waves, a unit in terms of *power* makes more sense in the frequency domain. With a known time window $T^w=\mathfrak{N}\triangle t$, the continuous-wave spectral

energy in this time window is $P_{\mathrm{CW}}(\omega)T^w = \frac{1}{2\pi C_{\mathfrak{F}}^2}|A_{\mathrm{CW}}(\omega)|^2$, where $P_{\mathrm{CW}}(\omega)$ is in "W / (rad · Hz)." Hence,

$$|A_{\mathrm{CW}}(\omega)| = C_{\mathfrak{F}}\sqrt{\overline{2\pi P_{\mathrm{CW}}(\omega)T^w}} = C_{\mathfrak{F}}\sqrt{\overline{P_{\mathrm{CW}}(\nu)T^w}}, \tag{S25}$$

by use of the relation $P_{\mathrm{CW}}(\nu) = 2\pi P_{\mathrm{CW}}(\omega)$. $P_{\mathrm{CW}}(\nu)$ is in W / Hz. This leads to, with Eq. (S15),

$$|A_{D,\mathrm{CW}}(\omega)| = \frac{C_{\mathfrak{F}_D}}{\triangle t}\sqrt{\overline{2\pi P_{\mathrm{CW}}(\omega)T^w}} = \frac{C_{\mathfrak{F}_D}}{\triangle t}\sqrt{\overline{P_{\mathrm{CW}}(\nu)T^w}}, \tag{S26}$$

which results in $|A_{D,\mathrm{CW}}(\omega)| = \sqrt{\overline{P_{\mathrm{CW}}(\nu)/T^w}} = \sqrt{\overline{P_{\mathrm{CW}}(\nu)}\triangle\nu}$ with the DFT convention we use here (note that $T^w = 1/\triangle\nu$).

In the common model of adding noise photon (e.g., shot noise), the noise is added as a CW background with one noise photon per frequency mode/bin, or equivalently, with an one-noise-photon spectral distribution (J = W / Hz) $P_{\mathrm{noise}}(\nu) = h\nu$ [10][11][12][13]. Eq. (S25) leads to

$$|A_{\text{noise photon}}(\omega)| = C_{\mathfrak{F}}\sqrt{\overline{T^w h\nu}} \tag{S27a}$$

$$|A_{D,\text{noise photon}}(\omega)| = \frac{C_{\mathfrak{F}_D}}{\triangle t}\sqrt{\overline{T^w h\nu}}, \tag{S27b}$$

Eq. (S27b) gives $|A_{D,\text{noise photon}}(\omega)| = \sqrt{\overline{h\nu/T^w}} = \sqrt{\overline{h\nu}\triangle\nu}$ with the DFT convention we use here.

The power spectral density $P(\omega)$ or $P(\nu)$ can also be represented in the wavelength domain. First, we derive the relation

$$\begin{aligned} & c = \nu\lambda \\ & \Rightarrow 0 = \lambda d\nu + \nu d\lambda \\ & \Rightarrow d\nu = -\frac{\nu}{\lambda}d\lambda = -\frac{c}{\lambda^2}d\lambda \end{aligned} \tag{S28}$$

which leads to

$$\begin{aligned} \int P(\lambda)|d\lambda| &= \int P(\nu)|d\nu| \\ &= \int P(\nu)\left|-\frac{c}{\lambda^2}d\lambda\right| = \int\left(\frac{c}{\lambda^2}P(\nu)\right)|d\lambda| \\ &\Rightarrow P(\lambda) = \frac{c}{\lambda^2}P(\nu) \end{aligned} \tag{S29}$$

Because wavelength and frequency have an inverse relation, and the power is always positive, an absolute value is taken in derivation. $P(\lambda)$ has the unit "J / m," whose CW version [Eqs. (S25) and (S26)] is in "W / m."

3. Discrete Fourier transform (DFT)

During operations of DFT in numerical computations, it is sometimes necessary to apply (MATLAB's) "fftshift" and "ifftshift," the offset of the signal. However, when and how to apply them, especially in different Fourier-transform conventions, can be confusing. Despite various conventions, fftshift is used to shift the signal to the center of the window (move $t_x = 0$ or $\nu_x = 0$ to window's center), whether it is in temporal or spectral domain. On the other hand, ifftshift is to cancel the fftshift effect and shifts the signal to center at $t_x = 0$ or $\nu_x = 0$(left edge of the window). t_x and ν_x represent the sampling coordinates in the temporal and spectral domains, respectively. It is important to note that the periodicity occurs for both temporal and spectral domains (Fig. S2). They should not be used simply as a pair of (fft,fftshift) and (ifft,ifftshift) due to different Fourier-transform conventions. For example, to compute the spectrum under the physical Fourier-transform convention ($c_s = 1$), we should follow (in MATLAB syntax below)

```
Nt = size(field,1); % the number of sampling points
t = (-Nt/2:Nt/2-1)'*dt; % ps; time coordinates; dt = temporal sampling spacing
c = 299792.458; % nm/ps; speed of light
f = f0+(-Nt/2:Nt/2-1)'/(Nt*dt); % THz; frequency coordinate; f0 = center frequency of the freuqnency window
wavelength = c./f; % nm
correct_unit = (Nt*dt)^2/1e3; % to make the spectrum of the correct unit "nJ/THz" [Eq.(S24)]
                              % "/1e3" is to make pJ into nJ
                              % "field" unit: sqrt(W)
spectrum = abs(fftshift(ifft(field),1)).^2*correct_unit; % nJ/THz; centered at the frequency window [Fig.S2(c)]
```

In practice, the time coordinate is placed such that the pulse at the center of the numerical time window locates at $t = 0$ in real-time (t) coordinates [Fig. S2(b)]. Do not confuse it with the pulse locating at $t_x = 0$ [Fig. S2(a)]. In principle, the time coordinate can be placed arbitrarily because numerical computations see only the sampling-point coordinate t_x or ν_x.

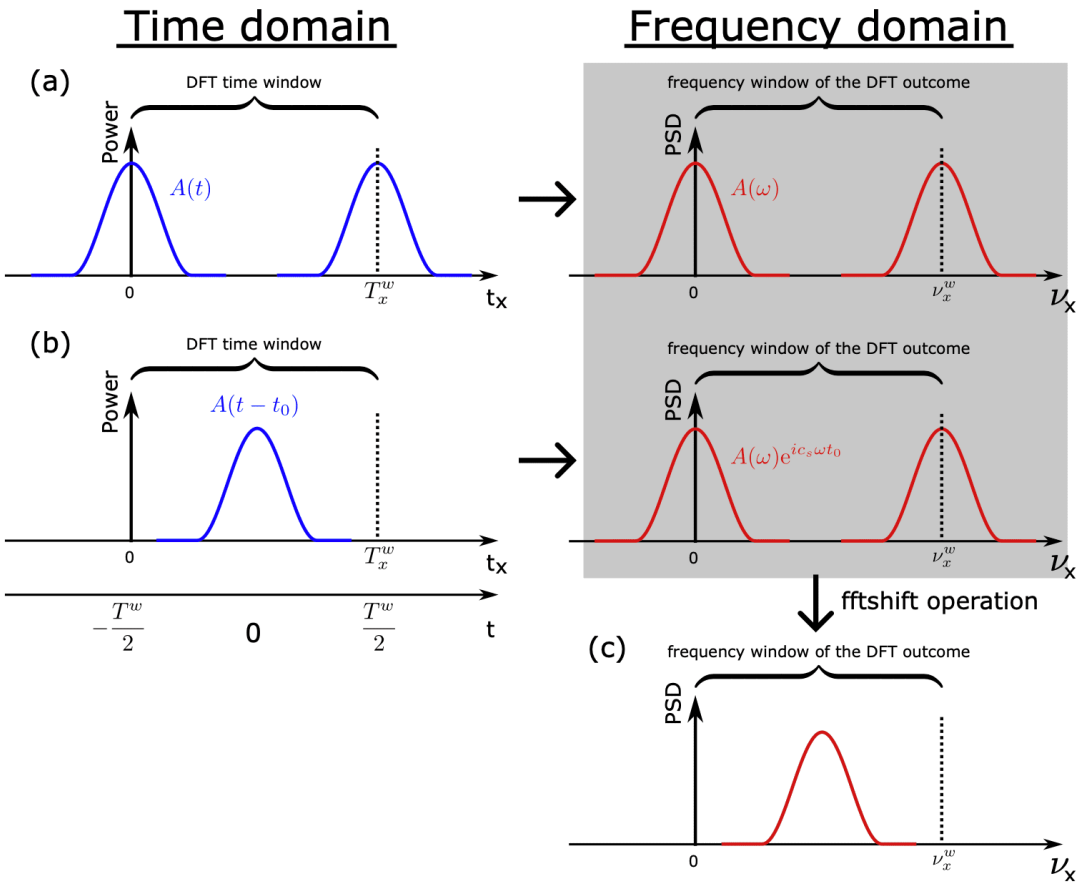

Figure S2. DFT conversion. (a) is the "formal" use of DFT when the temporal profile $|A(t)|^2$ is centered at $t = 0$. However, in numerical simulations, it is common to place the pulse at the center of the time window for visualization purpose (b), resulting in a spectral phase shift that doesn't affect the spectral shape. (c) is the result after fftshift centers the spectrum with respect to the frequency window. PSD: power spectral density $\sim |A(\omega)|^2$. Here, the subscript "x" represents the coordinate of sampling points, rather than the actual time and frequency coordinates.

Due to the numerical phase-unwrapping process, the temporal position of the pulse can affect the acquirement of a smooth phase relation $\phi(\omega)$. Numerically, phase of a complex number is found within the range of either $(0, 2\pi]$ or $(-\pi, \pi]$. Phase unwrapping is a process that removes the phase jump by adding multiples of $\pm 2\pi$ when the phase change between two data

points is larger than a threshold value, typically π[Fig. S3(a)]. This operation is crucial in phase computations, such as characterizing the second-order spectral phase $\frac{\mathrm{d}^2\phi}{\mathrm{d}\omega^2}$ in a pulse to determine the pulse-dechirping strategy (see Sec. 4). Therefore, it is important to unwrap the phase correctly such that it does not arbitrarily add multiples of $\pm 2\pi$ that distorts the phase relation $\phi(\omega)$. Phase unwrap can go wrong when the phase relation $\phi(\omega)$ changes too drastically beyond the threshold value. The unwrapping operation will attempt to reduce the variation, leading to a kink, followed by a slope of reverse sign due to continuous reduction of phase by $\pm 2\pi$ [Fig. S3(b)]. Since a temporal offset of a pulse adds a linear spectral phase $(c_s \omega t_0)$ [Fig. S2(b)], this extra addition might increase the rate of phase change and trigger the wrong unwrapping operation. As a result, in ultrafast optics, the fundamental principle is to first remove the temporal offset and place the pulse at $t_x = 0$ (left edge of the time window), as in Fig. 2(a), before applying any spectra-phase computations. The value of temporal offset is remembered to recover the pulse position after the operation if necessary. However, if the phase relation inherently shows a rapid phase change, as illustrated in Fig. 3(b), the only viable solution to accurately unwrap the phase is to enhance the spectral resolution, which necessitates extending the time window.

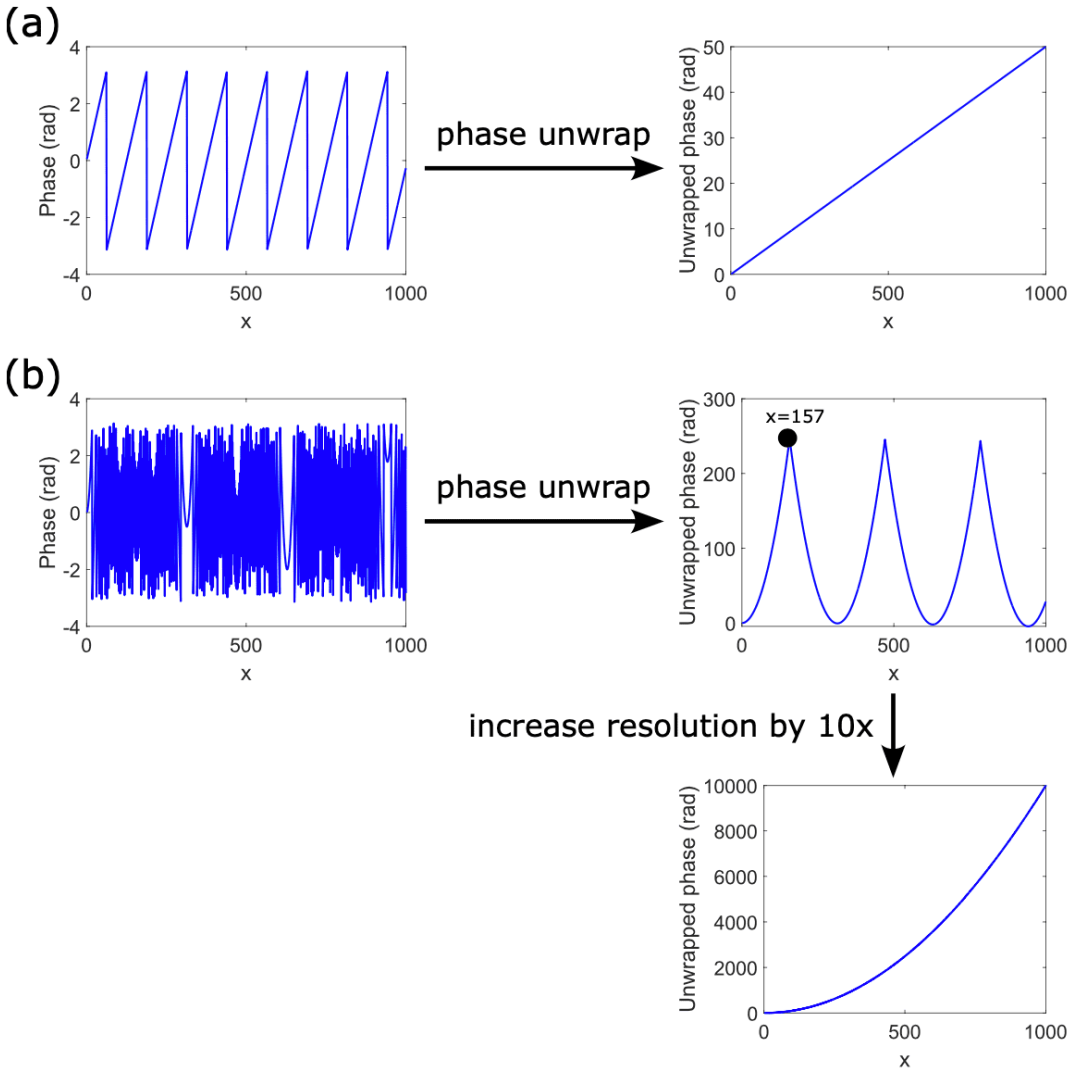

Figure S3. Phase-unwrapping process: $\phi(x) = \mathrm{unwrap}(\mathrm{angle}(y(x)))$ ($x = 0:1:1000$ here, integer array from 0 to 1000 in MATLAB syntax). In MATLAB, phase from $\mathrm{angle}(\cdot)$ is in $(-\pi, \pi]$. (a) Linear spectral phase: $y = e^{ix/20}$. Its phase does not vary dramatically between data points, so phase is correctly unwrapped. (b) Quadratic spectral phase: $y = e^{ix^2/100}$. This phase rapidly varies for larger values of x. Beyond $x = 157$, the phase change between two consecutive points always exceeds π, constantly triggering phase-unwrapping operation to add another -2π. This results in decreasing phase values, ultimately leading to the formation of multiple parabolic curves. To correctly unwrap the phase, the resolution is increased to 10 times: $x = 0:0.1:1000$ (from 0 to 1000 with 0.1 spacing).

Since in nonlinear optics, convolution is commonly used, such as in computations of Raman scattering[14,][4,], it is worth bringing it up again. Here, we use single-mode Raman scattering as an example, which has a term $\partial_z A(t) \propto A(t)\left(R(t) * |A(t)|^2\right)$ in limited conditions (e.g., ignoring the shock-wave effect, i.e., frequency dependence of nonlinearities). It follows

doi.org/10.32388/JFPRSL

$$
\begin{aligned}
R(t) * A(t)^2 &= \frac{1}{C_{\mathfrak{F}}} \mathfrak{F}^{-1}\left[\mathfrak{F}\left[R(t)\right] \mathfrak{F}\left[|A(t)|^2\right]\right] \quad \text{with Eq. (S10a)} \\
&= \frac{1}{C_{\mathfrak{F}}} \left(\frac{C_{\mathfrak{I}\mathfrak{F}}}{C_{\mathfrak{I}\mathfrak{F}_D}} \Delta\omega\right) \mathfrak{F}_D^{-1}\left[\left(\frac{C_{\mathfrak{F}}}{C_{\mathfrak{F}_D}} \Delta t \mathfrak{F}_D\left[R(t)\right]\right)\left(\frac{C_{\mathfrak{F}}}{C_{\mathfrak{F}_D}} \Delta t \mathfrak{F}_D\left[|A(t)|^2\right]\right)\right] \quad \text{with Eqs. (S13b) and (S15)} \\
&= \frac{\Delta t}{C_{\mathfrak{F}_D}} \mathfrak{F}_D^{-1}\left[\mathfrak{F}_D\left[R(t)\right] \mathfrak{F}_D\left[|A(t)|^2\right]\right] \quad \because \Delta t \Delta\omega = \frac{2\pi}{\mathfrak{N}}
\end{aligned} \tag{S30}
$$

In our convention ($C_{\mathfrak{F}_D} = \frac{1}{\mathfrak{N}}$), $R(t) * |A(t)|^2 = T^w \mathfrak{F}_D^{-1}\left[\mathfrak{F}_D\left[R(t)\right] \mathfrak{F}_D\left[|A(t)|^2\right]\right]$, where the time window $T^w = \mathfrak{N}\Delta t$. The factor of $\frac{\Delta t}{C_{\mathfrak{F}_D}}$ [Eq. (S30)] is important and can be easily forgotten.

4. Phenomena with complex-valued Fourier transform

Figs. S4 and S6 shows how the phase affects the signal. When the pulse has a flat phase in time domain, it is called "a transform-limited pulse." Its temporal and spectral width satisfy a fixed time-bandwidth product: a more-broadband pulse has a smaller duration. By adding a temporally (or spectrally) varying phase to the pulse, it modulates the signal. For example, adding a parabolic (second-order) phase to the temporal profile of a transform-limited signal creates a chirp, i.e., varying frequency at different temporal slices, broadening the spectrum [Fig. S4(b)]. The temporal frequency change follows $\Delta\omega(t) = \frac{1}{-c_s}\frac{d\phi}{dt}(t)$, so the phase effect to the signal is also dependent on the convention of Fourier transform. Similarly, adding a parabolic phase to the spectral profile increases the pulse duration, which is the "dispersion" effect: different frequencies moves at different speeds for a certain distance, widening the pulse's temporal profile [Figs. S4(c) and S5]. Fig. S6 shows the effect of a cubic phase, which broadens the spectral [Fig. S6(b)] or temporal [Fig. S6(c)] profiles with pedestals. Adding a linear chirp to the pulse to increase the pulse duration [Fig. S4(c)], reducing the peak power, is the basis of the chirp-pulse amplification[15] that was awarded the Nobel Prize in Physics in 2018. It enables amplification of an ultrashort pulse without suffering from significant nonlinear-phase accumulations due to a reduced peak power.

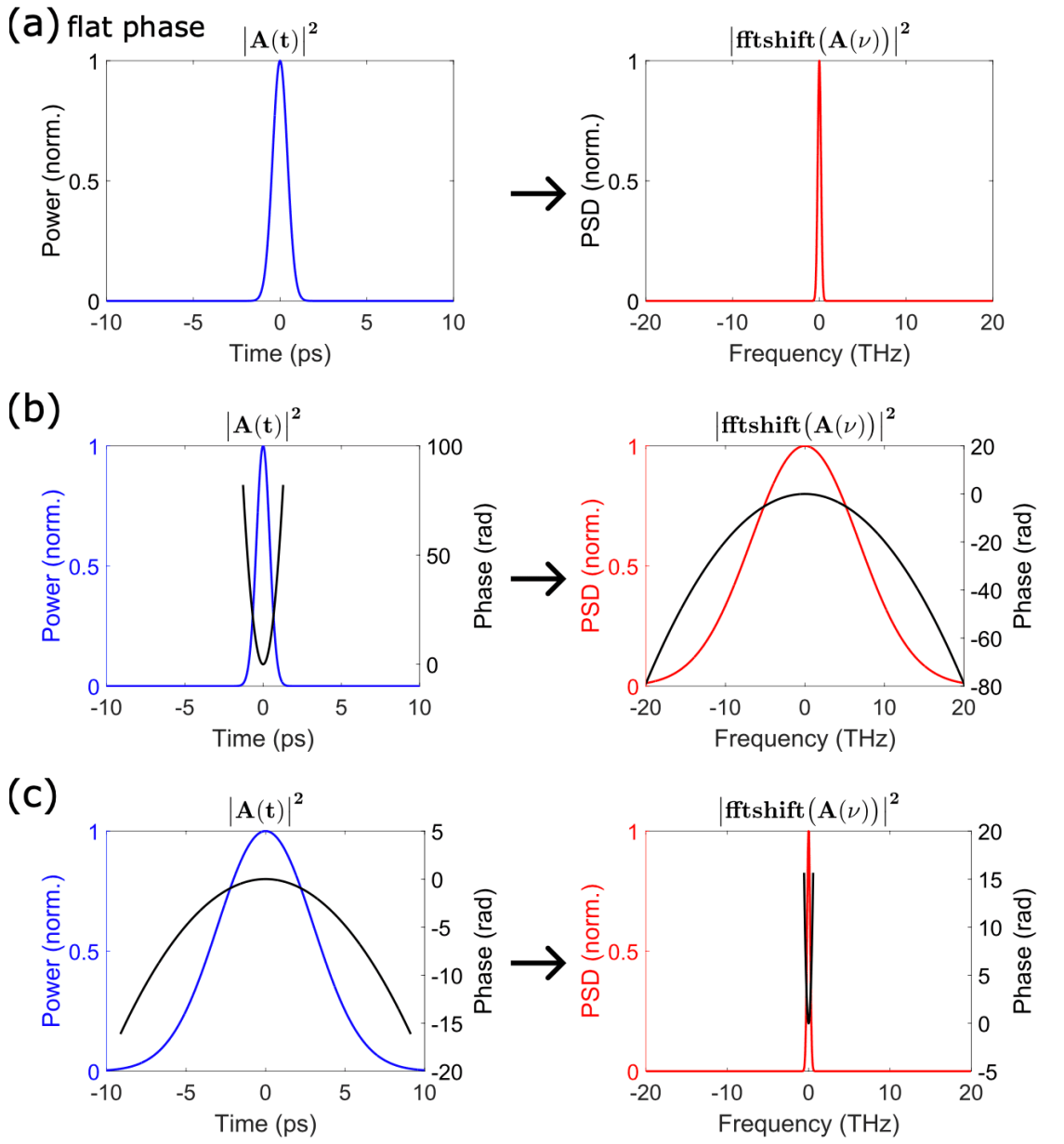

Figure S4. DFT conversion of a second-order chirped signal. (a) transform-limited pulse that has only flat phase in time domain. (b) and (c) add a parabolic phase to the temporal and spectral profiles, respectively.

doi.org/10.32388/JFPRSL

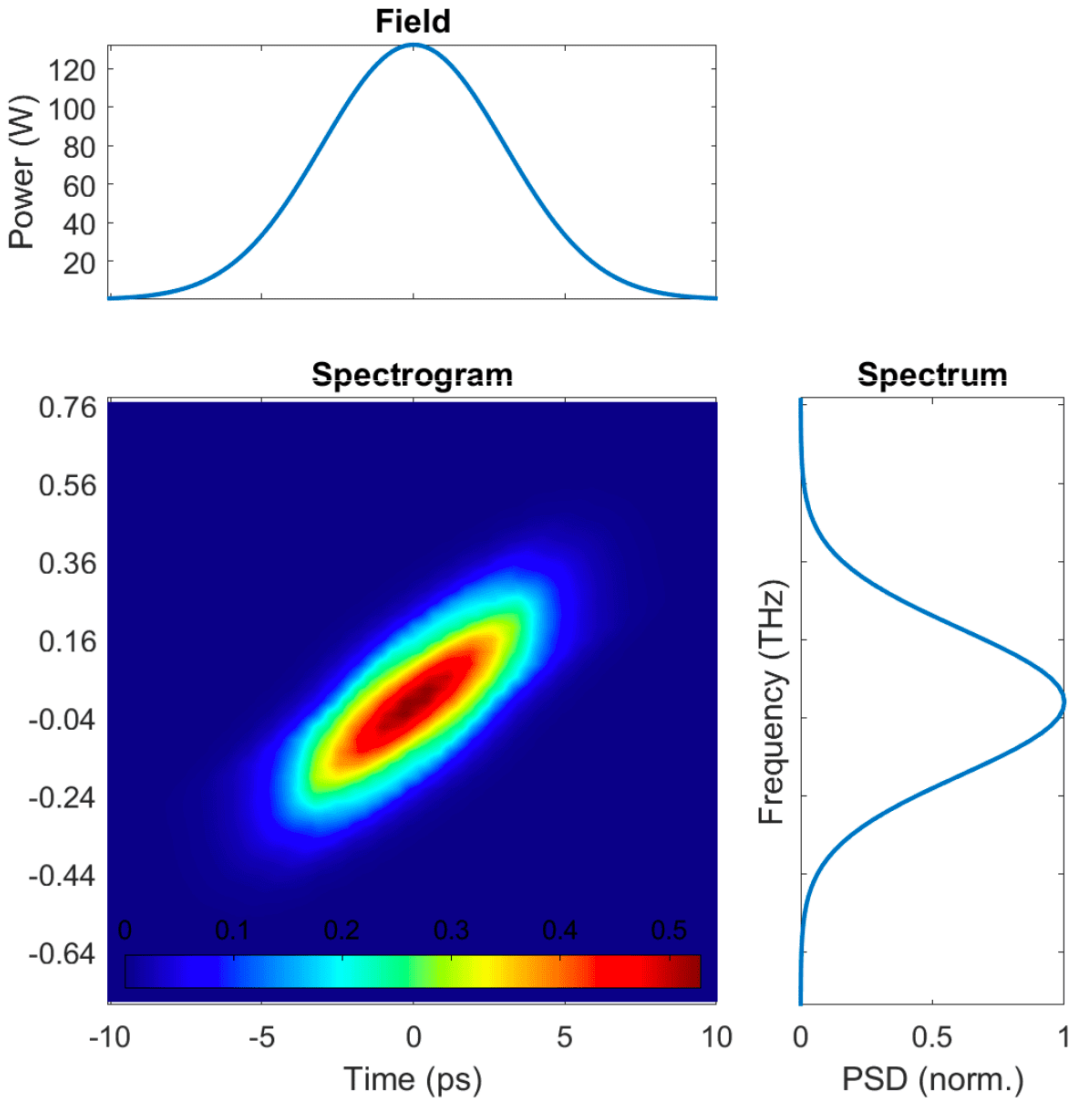

Figure S5. Spectrogram of a parabolically-chirped signal [Fig. S4(c)]. Here, the signal is positively-chirped such that lower-frequency components are in the temporal leading edge.

doi.org/10.32388/JFPRSL

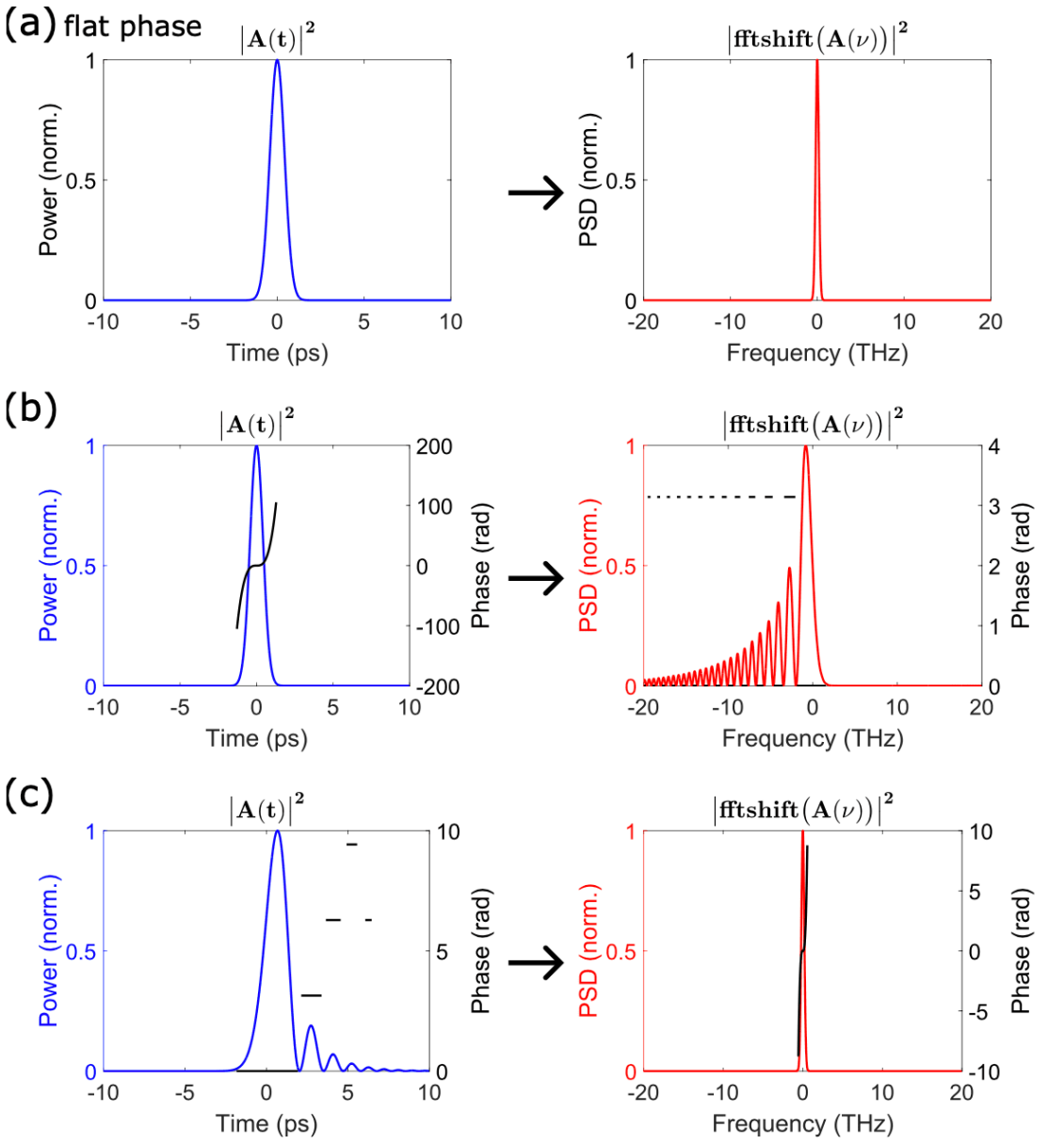

Figure S6. DFT conversion of a third-order chirped signal. (a) transform-limited pulse that has only flat phase in time domain. (b) and (c) add a cubic phase to the temporal and spectral profiles, respectively.

Footnotes

[1] A rule of thumb for the size of frequency window is that it needs to be around 5–10 times as the pulse bandwidth.

References

1. ^Boyd RW. Nonlinear Optics. 3rd ed. Burlington: Academic Press; 2008. ISBN 978-0-12-369470-6.

2. ^Conforti M, Marini A, Faccio D, Biancalana F (2013). "Negative frequencies get real: a missing puzzle piece in nonlinear optics". arXiv preprint arXiv:1305.5264. doi:10.48550/ARXIV.1305.5264. arXiv:1305.5264.
3. ^Chen YH, Varma S, York A, Milchberg HM. "Single-shot, space- and time-resolved measurement of rotational wavepacket revivals in H_2, D_2, N_2, O_2, and N_2O." Opt. Express. **15**(18):11341-11357 (2007). doi:10.1364/OE.15.011341. Available from: http://www.opticsexpress.org/abstract.cfm?URI=oe-15-18-11341.
4. a, b, cChen YH, Wise F (2024). "Unified and vector theory of Raman scattering in gas-filled hollow-core fiber across temporal regimes." APL Photonics. **9** (3): 030902. doi:10.1063/5.0189749.
5. ^Konyashchenko AV, Losev LL, Pazyuk VS, Tenyakov SY (2008). "Frequency shifting of sub-100 fs laser pulses by stimulated Raman scattering in a capillary filled with pressurized gas." Appl. Phys. B. **93** (2): 455–461. doi:10.1007/s00340-008-3177-1.
6. ^Chen YH, Moses J, Wise F. "Femtosecond long-wave-infrared generation in hydrogen-filled hollow-core fiber." J. Opt. Soc. Am. B. **40**(4):796-806 (2023). doi:10.1364/JOSAB.483969. Link to article.
7. ^Loree TR, Cantrell CD, Barker DL (1976). "Stimulated Raman emission at 9.2 μm from hydrogen gas". Opt. Commun.. **17** (2): 160–162. doi:10.1016/0030-4018(76)90204-2.
8. ^Grasyuk AZ, Losev LL, Nikogosyan DN, Oraevskii AA (1984). "Generation of single picosecond pulses of up to 0.6 mJ energy and of 9.2 μm wavelength by stimulated Raman scattering." Sov. J. Quantum Electron. **14** (9): 1257–1258. doi:10.1070/qe1984v014n09abeh006203.
9. ^Chen YH, Wise F (2024). "A simple accurate way to model noise-seeded ultrafast nonlinear processes." arXiv preprint arXiv: 2410.20567. Available from: https://arxiv.org/abs/2410.20567.
10. ^Eggleston J, Byer R (1980). "Steady-state stimulated Raman scattering by a multimode laser". IEEE J. Quantum Electron.. **16** (8): 850–853. doi:10.1109/JQE.1980.1070592.
11. ^Dudley JM, Genty G, Coen S (2006). "Supercontinuum generation in photonic crystal fiber". Rev. Mod. Phys.. **78** (4): 1135–1184. doi:10.1103/RevModPhys.78.1135.
12. ^Frosz MH (2010). "Validation of input-noise model for simulations of supercontinuum generation and rogue waves." Opt. Express. **18** (14): 14778–14787. doi:10.1364/OE.18.014778. Link.
13. ^Genier E, Bowen P, Sylvestre T, Dudley JM, Moselund P, Bang O (2019). "Amplitude noise and coherence degradation of femtosecond supercontinuum generation in all-normal-dispersion fibers." J. Opt. Soc. Am. B. **36**(2): A161--A167. doi:10.1364/JOSAB.36.00A161. Link to article.
14. ^Chen YH, Haig H, Wu Y, Ziegler Z, Wise F (2023). "Accurate modeling of ultrafast nonlinear pulse propagation in multimode gain fiber." J. Opt. Soc. Am. B. **40** (10): 2633--2642. doi:10.1364/JOSAB.500586. Link to article.
15. ^Strickland D, Mourou G (1985). "Compression of amplified chirped optical pulses." Optics Communications. **55** (6): 447–449. doi:10.1016/0030-4018(85)90151-8. Link to article.

Declarations

Funding: No specific funding was received for this work.

Potential competing interests: No potential competing interests to declare.